J Appl Electrochem (2014) 44:383–390
DOI 10.1007/s10800-013-0650-2

RESEARCH ARTICLE

Parametric studies of uranium deposition and dissolution at solid electrodes

Jinsuo Zhang

Received: 15 August 2013 / Accepted: 24 November 2013 / Published online: 7 December 2013

Abstract In pyroprocessing, most of uranium is separated from used nuclear fuel by depositing at a solid electrode of an electrorefiner. In the present study, a model, incorporating both diffusion and reaction kinetics of electrorefining, is developed. The model is applied to conduct parametrical studies on uranium deposition at an inert solid electrode to investigate properties of uranium deposition and dissolution and their dependence on the operating conditions. Both linear potential sweep and cyclic voltammetry processes are considered.

Keywords Modeling · Electrorefining · Pyroprocessing · Electrochemistry

1 Introduction

Pyroprocessing technology, originally developed by US for treatment of used metallic fuel [1], is being pursued by several nations, such as Japan, France, and South Korea [2]. The current research activities on pyroprocessing include the experimental demonstrations of industrial-scale applications and the development of plant-level simulation models [3]. However, most of the experimental measurements were conducted in electrochemical cells [4–6] under much simpler conditions than those encountered in the practical pyroprocessing [3], and most of the existing models [7–11] are based on the assumptions of diffusion control and reaction equilibriums. Therefore, fundamental studies on pyroprocessing, such as the development predictive models, are still needed.

Electrorefiner is the heart component of a pyroprocessing facility at where actinides are separated from fission products through electrofining [7]. The electrorefining process involves mass transfer, electrochemical, and chemical reactions. The available models based on diffusion control can take into account only physical processes such as mass transfer, while the chemical and electrochemical reactions are completely neglected. On the other hand, the assumption of reaction equilibria at an electrode results in the Nernst relationship between the electrode potential and the species concentration at the electrode surface, which leads to the ratio of concentration of two actinides (for example, plutonium and uranium) at an electrode being determined by the apparent potentials of the two ions [12]. For example, the potential of U/U^{3+} is $\sim$0.3 V more positive than thatof Pu/Pu^{3+} at 450 °C, which leads to the surface concentration of Pu^{3+} is $\sim 10^6$ times higher than that of U^{3+} at a solid electrode surface [7]. This outcome is impossible for anodic co-dissolution of Pu and U. Some existing model predicts artificial phenomena because of the assumption when it is applied to an electrorefiner, such as the very fast dissolution of all plutonium at a solid anode in a short period at the beginning of an operation, which is not consistent with experimental investigations [7]. The co-dissolution of Pu and U at an anode was modeled by adding an additional diffusion layer to the model based on diffusion control [13]. The model led to simulation results compatible with experimental results. However, the kinetics of theelectrochemical reactions was still not considered in the model. Most recently, the kinetics of U^{3+} reduction was taking into account using COMSOL commercial software [14], and the morphology of U deposition on cathode was simulated based on a

J. Zhang (✉)
Nuclear Engineering Program, The Ohio State University, 201 W 19th Avenue, Columbus, OH 43210, USA
e-mail: zhang.3558@osu.edu

phase-field simulation model [15]. The progresses in modeling indicate that simulation models can successfully simulate cyclic voltammetry (CV) profiles, polarization behaviors, and deposition morphologies.

In the present study, the previous model [10] is significantly improved by coupling mass transfer kinetics and electrochemical kinetics at the electrode surface. The new model can be applied to study the cases of diffusion control and diffusion-activation mixed control. The linear potential sweep and CV of UCl_3 in the molten KCl–LiCl are studied using the model to examine U dissolution and deposition behaviors at an inert solid electrode. Parametric studies are conducted. The simulation results indicate that the model is able to capture CV profiles of uranium that were reported experimentally. It is also able to capture some deposition features that cannot be effectively achieved by experiments, for example, the variations of the ion concentration at the electrode surface as a function of the operation time for a given initial condition.

2 Mathematic model development

In pyroprocessing, both U^{4+} and U^{3+} are stable in the molten KCl–LiCl [16]. The electrochemical reactions are:

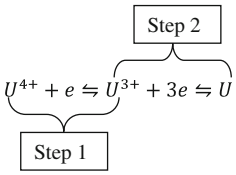

(1)

Therefore, the reduction of U^{4+} needs two steps as shown in the equation. Step 1 reaction belongs to the well-studied cases [17] of OX (oxidation state)/R (reduced state) occurred in solution with soluble–soluble exchange. While, Step 2 reaction results in U metal that deposits on the electrode surface. Therefore, the surface kinetics of Step 1 and Step 2 are different.

When the reactions are at equilibria, the potential at the electrode is expressed by:

$$\begin{aligned} E^{\mathrm{eq}} &= E^{0}_{\mathrm{U}^{4+}/\mathrm{U}^{3+}} + \frac{RT}{F}\ln\left(\frac{a_{\mathrm{U}^{4+}}}{a_{\mathrm{U}^{3+}}}\right) \\ &= E^{0}_{\mathrm{U}^{3+}/\mathrm{U}} + \frac{RT}{3F}\ln\left(\frac{a_{\mathrm{U}^{3+}}}{a_{\mathrm{U}}}\right), \end{aligned} \tag{2}$$

where E^{eq} is the equilibrium potential, E^0 is the standard potential which is calculated based on Gibbs free energy of the reaction, F is Faraday number (96,485 C mol^{-1}), R is gas constant (8.314 J mol^{-1} K^{-1}), T is temperature in kelvin, and a_i (i = U, U^{3+}, U^{4+}) is the activity of species i and can be expressed by:

$$a_i = \gamma_i x_i \tag{3}$$

with γ_i the activity coefficient and x_i the molar fraction. It is necessary to note that the activities of U^{3+} and U^{4+} are their activities in the molten salt, and the activity of U is its activity in the electrode at the electrode surface.

The apparent potential is defined as:

$$E^{\mathrm{ap}}_{\mathrm{U}^{4+}/\mathrm{U}^{3+}} = E^{0}_{\mathrm{U}^{4+}/\mathrm{U}^{3+}} + \frac{RT}{F}\ln\left(\frac{\gamma_{\mathrm{U}^{4+}}}{\gamma_{\mathrm{U}^{3+}}}\right), \tag{4}$$

$$E^{\mathrm{ap}}_{\mathrm{U}^{3+}/\mathrm{U}} = E^{0}_{\mathrm{U}^{3+}/\mathrm{U}} + \frac{RT}{3F}\ln\left(\frac{\gamma_{\mathrm{U}^{3+}}}{\gamma_{\mathrm{U}}}\right). \tag{5}$$

Then Eq. 2 can be rewritten as:

$$\begin{aligned} E^{\mathrm{eq}} &= E^{\mathrm{ap}}_{\mathrm{U}^{4+}/\mathrm{U}^{3+}} + \frac{RT}{F}\ln\left(\frac{x_{\mathrm{U}^{4+}}}{x_{\mathrm{U}^{3+}}}\right) \\ &= E^{\mathrm{ap}}_{\mathrm{U}^{3+}/\mathrm{U}} + \frac{RT}{3F}\ln\left(\frac{x_{\mathrm{U}^{3+}}}{x_{\mathrm{U}}}\right). \end{aligned} \tag{6}$$

For equilibrium cases, the current due to the electrochemical reaction is zero. For non-equilibrium cases, there is an overpotential which is defined as:

$$\eta = E - E^{\mathrm{eq}}. \tag{7}$$

If $\eta < 0$, the reaction will move forward, if $\eta > 0$, the reaction will move backward, and if $\eta = 0$, the reaction will be at its equilibrium state. The current density produced by the reaction can be expressed by the Butler–Volmer equation:

$$\begin{aligned} i_1 = Fk_1^0\Bigg[&c^s_{\mathrm{U}^{3+}}\exp\left(\frac{\alpha_1 n_1 F\eta_1}{RT}\right) \\ &-c^s_{\mathrm{U}^{4+}}\exp\left(-\frac{(1-\alpha_1)n_1F\eta_1}{RT}\right)\Bigg], \end{aligned} \tag{8}$$

$$\begin{aligned} i_2 = 3Fk_2^0\Bigg[&\sigma c^s_{\mathrm{U}}\exp\left(\frac{\alpha_2 n_2 F\eta_2}{RT}\right) \\ &-c^s_{\mathrm{U}^{3+}}\exp\left(-\frac{(1-\alpha_2)n_2F\eta_2}{RT}\right)\Bigg], \end{aligned} \tag{9}$$

where η_1 and η_2 are defined by:

$$\eta_1 = E - E^{\mathrm{ap}}_{\mathrm{U}^{4+}/\mathrm{U}^{3+}},\ \eta_2 = E - E^{\mathrm{ap}}_{\mathrm{U}^{3+}/\mathrm{U}}. \tag{10}$$

The superscript s represents the surface of the electrode, and c represents the concentration. $c^s_{U^{3+}}$ and $c^s_{U^{4+}}$ are in mol cm^{-3}, while c^s_U is in mol cm^{-2}. k^0_j $(j = 1, 2)$ is the standard rate constant with a unit of cm s^{-1}, and σ is the ratio of the forward constant to the backward constant for Step 2 reaction. σ has unit of cm^{-1}. In the present model, the ratio is set to be 1 cm^{-1} for all the calculations.

Based on Eqs. 8 and 9:

$$i_1 = Fk_1^0\left[c^s_{\mathrm{U}^{3+}} - c^s_{\mathrm{U}^{4+}}\right], \tag{11}$$

when $\eta_1 = 0$, and

$$i_2 = 3Fk_2^0\left[\sigma c_{\mathrm{U}}^s - c_{\mathrm{U}^{3+}}^s\right] \quad (12)$$

when $\eta_2 = 0$.

The rates of the formation of the uranium ions and uranium metal at the electrode surface by the electrochemical reactions can be expressed by:

$$R_{2,\mathrm{U}} = -\frac{i_2}{3F}, \quad (13)$$

$$R_{2,\mathrm{U}^{3+}} = -R_{2,\mathrm{U}}, \quad (14)$$

for Step 2, and:

$$R_{1,\mathrm{U}^{3+}} = -\frac{i_1}{F}, \quad (15)$$

$$R_{1,\mathrm{U}^{4+}} = -R_{1,\mathrm{U}^{3+}} \quad (16)$$

for Step 1.

Uranium cannot dissolve into the molten salt (LiCl–KCl) in its metal form. Therefore, only the mass transfer of the uranium ions (U^{3+} and U^{4+}) in the molten salt needs to be taken into account. Considering static and one-dimensional cases, the mass transfer of ions in the molten salt is determined by the diffusion which can be expressed by:

$$\frac{\partial c_{\mathrm{U}^{n+}}}{\partial t} = D_{\mathrm{U}^{n+}}\frac{\partial^2 c_{\mathrm{U}^{n+}}}{\partial^2 x}, \quad (17)$$

where $n = 3$ or 4, $D_{\mathrm{U}^{n+}}$ is the diffusion coefficient of the ion in the molten salt, and x is the coordinate along the normal direction of the electrode surface. The ion flux rate ($R_{\mathrm{m},\mathrm{U}^{n+}}$) to/from the electrode surface can be expressed by:

$$R_{\mathrm{m},\mathrm{U}^{n+}} = -D_{\mathrm{U}^{n+}}\frac{\partial c_{\mathrm{U}}^{n+}}{\partial x}\Big|_{x=0}, \quad (18)$$

The current density due to mass transfer of an ion is calculated by:

$$i_{\mathrm{m}} = -nFR_{\mathrm{m},\mathrm{U}^{n+}}. \quad (19)$$

Both kinetics of mass transfer and electrochemical reactions at the electrode surface must be considered. They can be coupled together by modeling the boundary conditions. For U^{3+} and U^{4+}, their concentrations at the surface can be calculated by:

$$\delta_l\frac{\partial c_{\mathrm{U}^{n+}}}{\partial t} = R_{1,\mathrm{U}^{n+}} + R_{2,\mathrm{U}^{n+}} + R_{\mathrm{m},\mathrm{U}^{n+}}, \quad (20)$$

where δ_1 is the thickness of the surface layer.

For uranium metal on the electrode, the uranium activity at the surface should be in the range of 0–1 [18]. In the present model, it is assumed that the activity is 1 when the solid electrode is fully covered by uranium, and the activity equals to the covered fraction when the surface is partially covered by uranium, and the concentration (mol cm^{-2}) at the surface of a solid electrode is calculated by:

$$\frac{\partial c_{\mathrm{U}}}{\partial t} = R_{2,\mathrm{U}} \quad (21)$$

which is based on an assumption of all depositing uranium contacting with molten salt.

3 Results and discussion

For conducting calculations using the model, the apparent potentials of the electrochemical reactions, the diffusion coefficients of U^{3+} and U^{4+} in the molten salt, and the standard constants, k_j^0, must be identified. For the potentials and diffusion coefficients, extensively measured data have been reported. The most recent data were reviewed and re-analyzed [16], and temperature-depended-correlations were developed based on the existing experimental measurements [16]:

$$E^{\mathrm{ap}}_{\mathrm{U}^{3+}/\mathrm{U}} = -2.9429 + 5.8724 \times 10^{-4}T$$

$$E^{\mathrm{ap}}_{\mathrm{U}^{4+}/\mathrm{U}^{3+}} = -1.669 + 2.1 \times 10^{-4}T$$

$$D_{\mathrm{UCl_3}} = 2.291 \times 10^{-3}\exp\left(-\frac{32550}{RT}\right)$$

$$D_{\mathrm{UCl_4}} = 3.467 \times 10^{-3}\exp\left(-\frac{37450}{RT}\right)$$

In the above correlations, the temperature is in kelvin, the potential (vs. $\mathrm{Cl^-/Cl_2}$, without addition note, all the potentials in this article are referenced to $\mathrm{Cl^-/Cl_2}$), is in voltage, and the diffusion coefficient is in $\mathrm{cm^2\ s^{-1}}$.

For the standard constant, k_j^0, the constant is estimated through comparing potential-current profiles of CV processes obtained by the present model with results obtained by experiments reported [4, 6]. When it uses $k_1^0 = k_2^0 = 0.001$ cm $\mathrm{s^{-1}}$, the profiles obtained by the model (given in Fig. 1) are very close to the profiles by experiments [4, 6]. Therefore, for all the simulations in the present article, the constants were selected to be 0.001 cm $\mathrm{s^{-1}}$ which is in the same order of the rate of U^{4+} reduction and one order larger than the rate of U^{3+} reduction reported [19] and in the range given in Ref. [20]. For improving the calculation accuracy, the more accurate data are needed which can be obtained by future experiments or first principle simulations [21].

Figures 1 and 2 show the CV profiles of $\mathrm{UCl_3}$–LiCl–KCl with an initial $\mathrm{UCl_3}$ concentration, $c^i_{\mathrm{U}^{3+}}$, 9.87×10^{-5} mol $\mathrm{cm^{-3}}$ for different scan rates. The applied potential scans from −3 to −1 V for Fig. 1 and from −2 to −1 V for Fig. 2. The dashed-line arrows in the figures show the scan directions. The two figures indicate that the present model can capture the main features of the dissolution and deposition of U at an inert solid electrode in a $\mathrm{UCl_3}$–LiCl–KCl salt with diluted $\mathrm{UCl_3}$ which have been reported experimentally by different authors (e.g., Refs. [4, 6]). Two pairs of peaks ($I_c^1 - I_a^1$ and $I_c^2 - I_a^2$) are

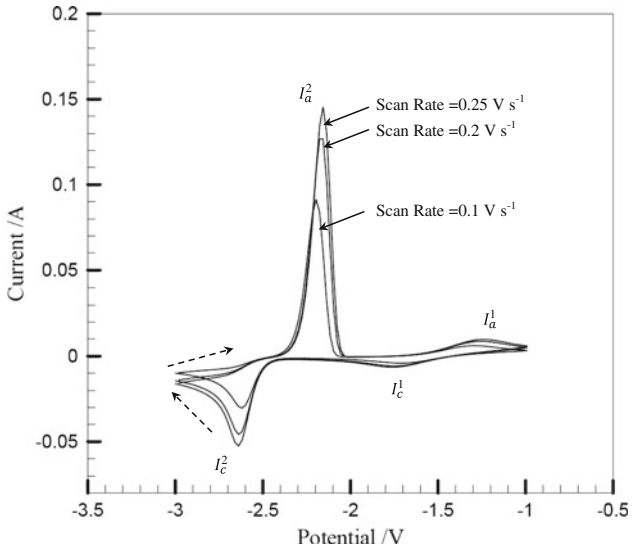

Fig. 1 Cyclic voltammetry of the U^{3+}/U system for different potential scan rates at 773 K, the surface area $S = 0.34$ cm^2, $c^i_{U^{3+}} = 9.87 \times 10^{-5}$mol cm^{-3}, $c^i_{U^{4+}} = 0.0$

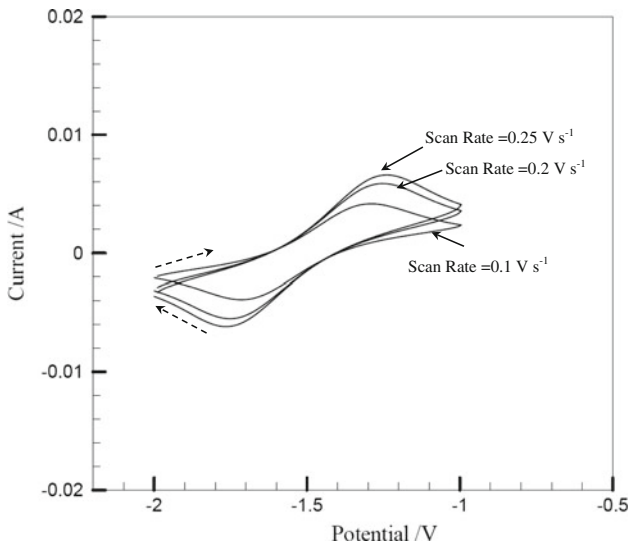

Fig. 2 Cyclic voltammetry of the U^{4+}/U^{3+} system for different potential scan rates at 773 K, the surface area $S = 0.34$ cm^2, $c^i_{U^{3+}} = 9.87 \times 10^{-5}$mol cm^{-3}, $c^i_{U^{4+}} = 0.0$

obtained. $I_c^1 - I_a^1$ corresponds to Step 1 as given in Eq. 1, and $I_c^2 - I_a^2$ corresponds to Step 2. There is another pair of peaks by experiments [6] that is not captured by the present model. According to the reference, the third pair of peaks corresponds to the adsorption of U^{3+} at the solid electrode. The present model does not consider the adsorption effects. Therefore, the present model cannot capture the third pair of peaks.

Both Figs. 1 and 2 indicate that changing the scan rate does not lead to CV profile change, but does result in the

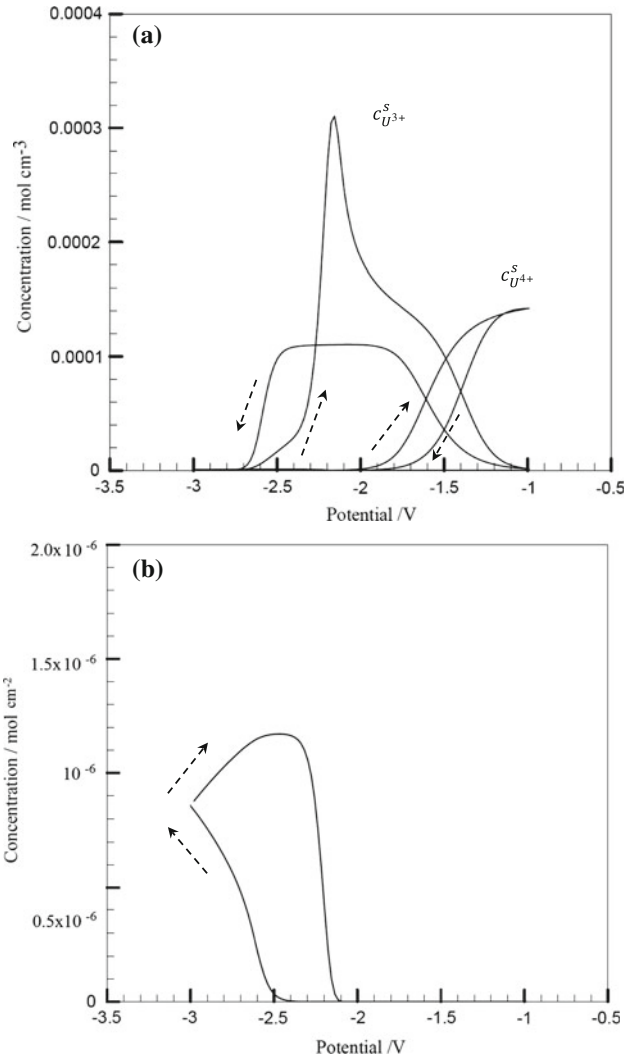

Fig. 3 Surface concentrations for a cyclic voltammetry process with a scan rate of 0.1 V s^{-1} at 773 K, $S = 0.34$ cm^2, $c^i_{U^{3+}} = 9.87 \times 10^{-5}$mol cm^{-3}, $c^i_{U^{4+}} = 0.0$. **a** Surface concentration of U^{3+} and U^{4+}. **b** Surface concentration of U

changes of the values of the current peaks. The absolute values of the current peaks increase with the scan rate increasing. However, the potential at which the peak appears does not change with the scan rate increasing. All these phenomena are common for a general CV process, and have been revealed by experiments on studying U behaviors in molten salt (e.g., Refs. [4, 6], more reference in the review article [16]), which is used to validate the present model. The present model not only can predict the phenomena that have been already found experimentally, but also can predict some features that cannot or are very difficult to be measured by experiments, for example, the surface concentrations of species (ions and metal) involved. Figure 3 shows the surface concentrations of U^{3+}, U^{4+} and metal U.

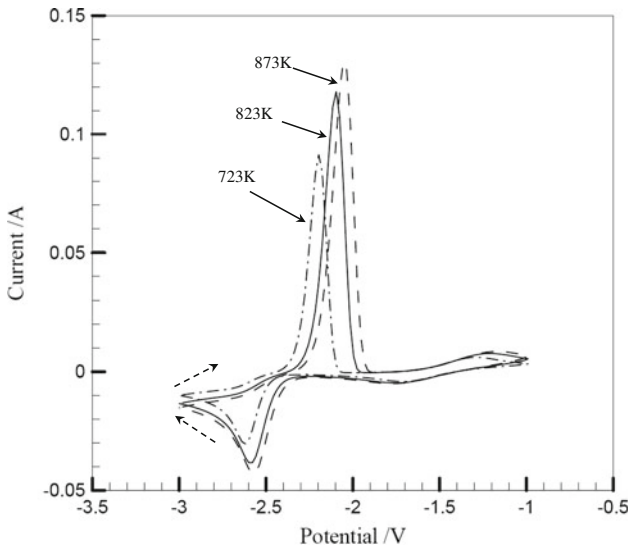

Fig. 4 Cyclic voltammetry profiles for different temperatures with a scan rate of 0.1 V s^{-1}, $S = 0.34$ cm^2, $c^i_{U^{3+}} = 9.87 \times 10^{-5}$mol cm^{-3}, $c^i_{U^{4+}} = 0.0$

The concentration profiles (Fig. 3) can provide information on the materials transport from/to the electrode surface. When it scans forward from -3 to -1 V, the concentration of U^{3+} starts to increase with a slow rate after some operation time; then, the rate becomes larger, and the concentration reaches its peak value. The change of the concentration in this period occurs, because the electrochemical Step 2 reaction, $U^{3+} + 3e \leftrightharpoons U$, is backward (that is, the dissolution of U metal). After the peak value is reached, the concentration of U^{3+} starts to decrease and continues decreasing after it reaches the value of the bulk concentration, because U^{3+} is converted to U^{4+} due to Step 1 reaction, $U^{4+} + e \leftrightharpoons U^{3+}$, which is also backward. Therefore, the surface concentration of U^{4+} starts to increase from a value which is almost zero, and the diffusion of U^{4+} from electrode surface to the bulk molten salt occurs. The non-zero current as shown in Fig. 2 is due to the diffusion of U^{4+} from the electrode surface to the bulk. When it scans backward from -1 to -3 V, the concentration of U^{3+} at the electrode surface increases and that of U^{4+} decreases, because Step 1 reaction is forward, $U^{4+} + e \rightarrow U^{3+}$, which produces U^{3+} and consumes U^{4+}. With the potential decreasing, the surface concentration of U^{3+} approaches to the bulk concentration and stays there for a while and that of U^{4+} approaches to zero as shown in the figure. Since there is no concentration gradient from bulk to the surface, there is no current in this range as shown in Fig. 1. When it scans backward further, the surface concentration of U^{3+} decreases, because Step 2 reaction is forward, $U^{3+} + 3e \rightarrow U$, which consumes U^{3+} and results in a mass flow of U^{3+} from the bulk to the surface. For U metal, when it scans forward, the surface concentration increases first due to the U^{3+} deposition; then, there is a sudden decrease due to U dissolution. When it scans backward, the concentration starts to increase when the potential is more negative than the equilibrium potential of the corresponding electrochemical reaction.

Temperature is one of the most important parameters for studying U dissolution and deposition in a molten salt system. The effects of operating temperatures on the CV profiles are shown in Fig. 4. The figure indicates that increasing temperature does not affect the profile shape but moves the peak potential to the positive direction. The peak values also increase with the temperature increasing. These effects can be explained when it is taken into account that the apparent potential moves to the positive direction and the diffusion coefficient increases when the operating temperature increases.

For studying the effects of the initial conditions of the molten salt, two initial conditions are selected: Condition 1: $c^i_{U^{3+}} = 9.87 \times 10^{-5}$mol cm^{-3}, $c^i_{U^{4+}} = 0.0$, and Condition 2: $c^i_{U^{3+}} = 0.0$, $c^i_{U^{4+}} = 9.87 \times 10^{-5}$mol cm^{-3}. The results for linear potential with different scanning directions for the two initial conditions are given in Figs. 5 and 6, respectively. For better understanding the mass flow of U^{3+} and U^{4+}, the currents due to the diffusion in the molten salt of the two ions are also shown in the two figures.

For Condition 1 when it scans from -3 V to the positive direction, both of Step 1 and Step 2 reactions move forward at the beginning, because the initial potential is more negative than the apparent potentials of both Step 1 and Step 2 reactions. However, there is no U^{4+} in the molten salt at the beginning, and Step 1 reaction won't happen. For this initial condition, the current by U^{4+} diffusion is zero as shown in Fig. 5a at the beginning, and the overall current is dominated by Step 2 reaction which depends on the diffusion of U^{3+}. The overall current profile is very similar to the profile of the current U^{3+} diffusion until the potential reaches a point at where Step 1 reaction moves backward. The backward Step 1 reaction produces U^{4+} and consumes U^{3+}, which results in diffusion of U^{4+} from the electrode surface and diffusion of U^{3+} to the electrode surface. After the point, the current from the electrode due to U^{4+} diffusion and the current to the electrode due to U^{3+} diffusion increase when the potential moves to the more positive direction with a linear sweep rate, and both of the currents together with the overall current reach peak values, and then decrease with the potential.

For Condition 1 when it scans from -0.5 V to the negative direction, both Step 1 and Step 2 reactions move backward. However, considering that there is no U on the inert electrode initially, the backward Step 2 reaction won't happen. Therefore, at the beginning, the only reaction that produces current is $U^{4+} + e \leftarrow U^{3+}$ which consumes U^{3+}

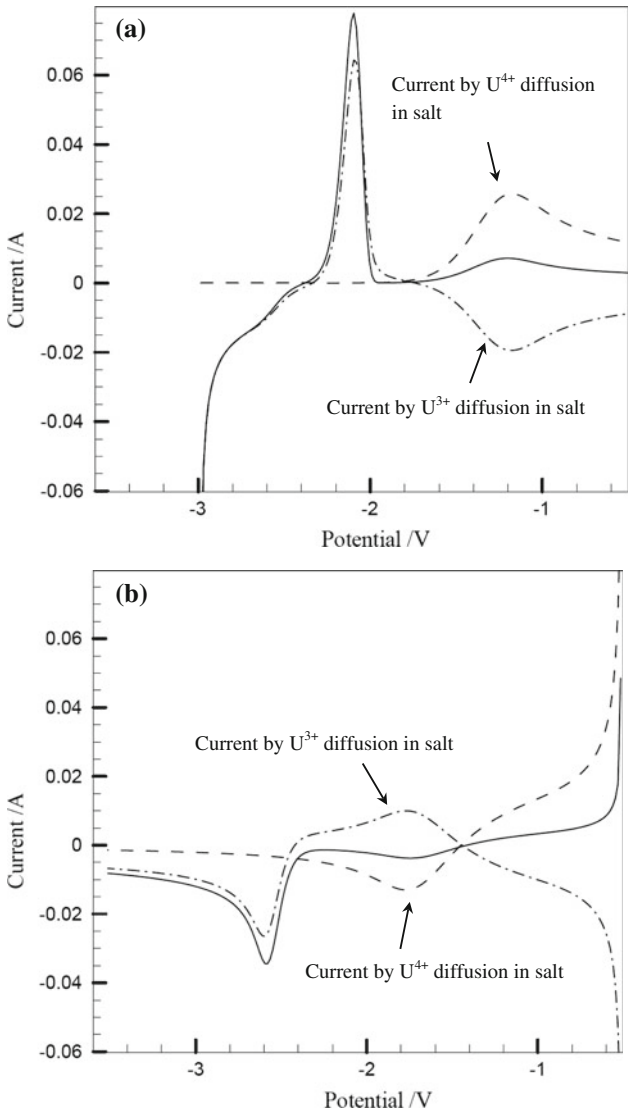

Fig. 5 Current profiles for a linear potential sweep with a scan rate of 0.1 V s^{-1} at 823 K for initial Condition 1, $S = 0.34$ cm^2, *solid line* represents the overall current. **a** Scan from −3 V to positive direction. **b** Scan from −0.5 to negative direction

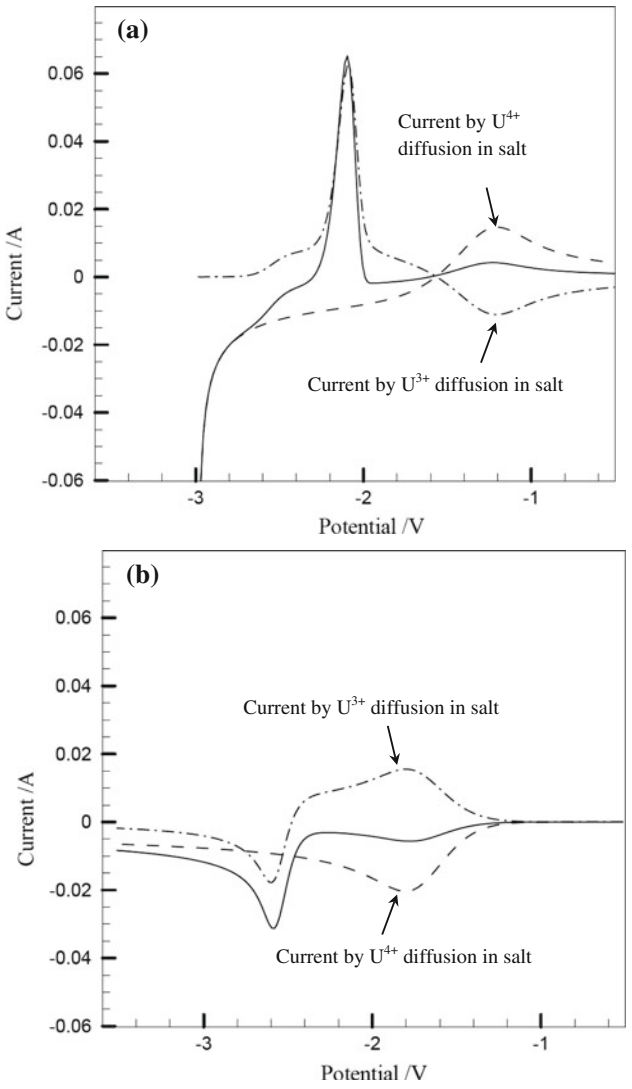

Fig. 6 Current profiles for a linear potential sweep with a scan rate of 0.1 V s^{-1} at 823 K for initial Condition 2, $S = 0.34$ cm^2, *solid line* represents the overall current. **a** Scan from −3 V to positive direction. **b** Scan from −0.5 V to negative direction

and produces U^{4+} at the electrode surface. As shown in Fig. 5b, U^{4+} diffuses from the surface to the bulk, while U^{3+} diffuses from the bulk to the electrode surface at the beginning. Both of the currents due to U^{4+} diffusion (from the electrode surface, positive) and due to U^{3+} diffusion (to the electrode surface, negative) together with the overall current decrease with the applied potential moving to the more negative direction until Step 1 reaction moves forward. Then, the current due to U^{4+} diffusion becomes negative and that due to U^{3+} diffusion becomes positive. After the peak potential, the current due to U^{4+} diffusion approaches to zero from its negative peak, while the current due to U^{3+} diffusion together with the overall current approaches to a negative peak which corresponds to Step 2 reaction $U^{3+} + 3e \rightleftharpoons U$. After the peak potential, all types of the currents approach to zero due to diffusion control.

For Condition 2, when it scans from −3 V to the positive direction, both Step 1 and Step 2 reactions occur and move forward even if there is no initial U^{3+} in the molten salt. Most of the U^{3+} produced by Step 1 reaction is converted to U by Step 2 reaction at the beginning as shown in Fig. 6a. When the dissolution of U starts to occur or Step 2 reaction moves backward, the current profiles for Condition 2 are similar to these for Condition 1. For Condition 2 when it scans from −0.5 V to the negative direction, there is no current at the beginning because of no electrochemical reaction at the electrode interface as shown in Fig. 6b which is significantly different from Condition 1. When

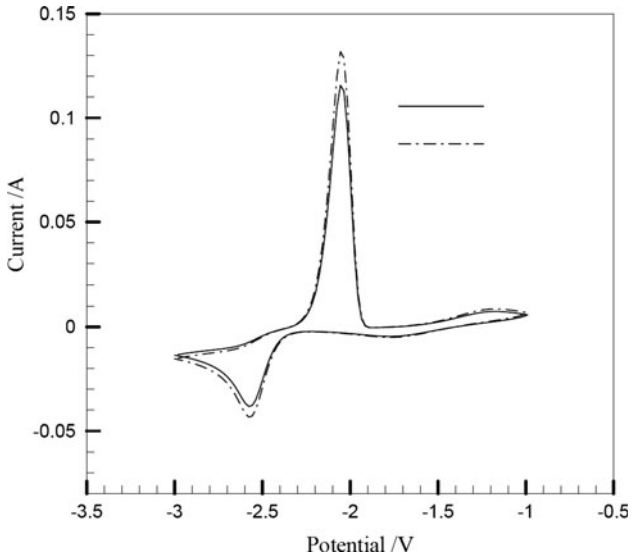

Fig. 7 Cyclic voltammetry profiles with a scan rate of 0.1 V s^{-1} at 823 K for different initial conditions, $S = 0.34$ cm^2, *solid line* $c^i_{U^{3+}} = 0.0$, $c^i_{U^{4+}} = 9.87 \times 10^{-5}$mol cm^{-3}, and *dashed line* $c^i_{U^{3+}} = 9.87 \times 10^{-5}$mol cm^{-3}, $c^i_{U^{4+}} = 0.0$

Step 1 reaction starts to move forward with the potential moving to the more negative direction, the current profiles become similar to these of Condition 1.

The CV current profiles for the both initial conditions are given in Fig. 7. The figure indicates that the initial conditions with the same amount of U in the molten salt do not have significant effects on U deposition and diffusion for CV processes.

4 Conclusion

In the present study, an activation–diffusion mixed controlled model for the two-step electrochemical reaction of U deposition and dissolution in molten LiCl–KCl was developed. The model was applied to study the CV and linear potential sweep processes of a molten salt of LiCl–KCl solution with UCl_3 and UCl_4 dissolved. The model successfully simulated the curves of current as a function of the applied potential which have been experimentally measured. The model could also capture other U dissolution and deposition features which have not been measured because of technical difficulties, such as the surfaces concentrations of U ions and metal at an inert solid electrode. The model can identify the partial currents due to diffusion of different U ions and the two-step U^{4+} reduction electrochemical reactions and their contributions to the overall current. Parametric studies showed the effects of operating temperatures, scan rates, and initial conditions.

Compared with existing models for pyroprocessing most of which were based on the assumptions of diffusion control and reaction equilibriums, the present model incorporates the kinetics of electrochemical reactions encountered in electrorefining U. Therefore, the model can be applied to study non-equilibrium and mix-controlled cases. However, the model still does not include the effects of adsorption and nucleation at the solid electrode. More advanced models are needed for fully understanding the electrorefining in the applications of pyroprocessing.

References

1. Goff KM, Simpson MF (2009) Dry processing of used nuclear fuel, Gobal 2009, INL/CON-09-15984
2. (2004) Pyrochemical separations in nuclear applications. A Status Report, NEA No. 5427
3. (2010) National programs in chemical partitioning. A Status Report, nuclear energy agency, organization for economic co-operation and development, NEA No. 5425, ISBN 978-64-99096-8
4. Kuznetsov SA, Hayashi H, Minato K, Ganue-Escard M (2005) Determination of uranium and rate-earth metals separation coefficients in LiCl–KCl melt by electrochemical transient techniques. J Nucl Mater 344:169–172
5. Martinot L, Duyckaerts G (1977) Diffusion of uranium species in several molten chlorides. Inorg Nucl Chem Lett 13:321–327
6. Masset P, Bottomley D, Konings R, Malmbeck R, Rodrigues A, Serp J, Glatz J (2005) Electrochemistry of uranium in molten LiCl–KCl Eutectic. J Electrochem Soc 152:A1109–A1115
7. Zhang J (2011), Echem Modeling: A kinetic model for electrorefining based on diffusion control, Los Alamos National Laboratory Report LA-UR-11-05276
8. Kobayashi T, Tokiwai M (1993) Development of trail, a simulation code for the molten salt electrorefining of spent nuclear fuel. J Alloy Compd 197:7–16
9. Kobayashi T et al (1995) Polarization effects in the molten salt electrorefining of nuclear fuel. J Nucl Sci Technol 32:653–663
10. Zhang J (2014a) Kinetic model for electrorefining, part I: model development and validation. Prog Nucl Energy 70:279–286
11. Zhang J (2014b) Kinetic model for electrorefining, part II: model application, Prog Nucl Energy 70:287–297
12. Pyrometallurgical processing research programme (2003) Contract FIKW-CT-2000-00049, final Report
13. Iizuka M, Kinoshita K, Koyama T (2005) Modeling of anodic dissolution of U–Pu–Zr ternary ally in the molten LiCl–KCl electrolyte. J Phys Chem Solids 66:427–432
14. Kim SH, Park SB, Lee SJ, Kim JG, Lee HS, Lee JH (2013) Computer-assisted design and experimental validation of multi-electrode electrorefiner for spent nuclear fuel treatment using a tertiary model. Nucl Eng Des 257:12–20
15. Shibuta Y, Sato T, Suzuki T, Ohta H, Kurata M (2013) Morphology of uranium electrodeposits on cathode in electrorefining process: a phase-field simulation. J Nucl Mater 436:61–67
16. Zhang J (2013) Electrochemistry of actinides and fission products in molten salts-data review, J Nucl Mater (in press)
17. Martinet S, Bouteillon J, Caire JP (1998) Modeling of cyclic voltammograms for two-step metal deposition on an inert electrode with adsorption. J Appl Electrochem 28:819–825
18. Noel M, Vasu KI (1990) Cyclic voltammetry and the frontiers of electrochemistry. Oxford & IBH Publishing Co. Pvt. Ltd., New Delhi

19. Kuznetsov SA, Hayashi H, Minato K, Gaune-Escard M (2005) Electrochemical behavior and osme thermodynamic properties of UCl_4 and UCl_3 dissolved in a LiCl–KCl eutectic melt. J Electrochem Soc 152:C203–C212
20. Kim GY, Yoon D, Paek S, Kim SH, Kim TJ, Ahn DH (2012) A study on the electrochemical deposition behavior of uranium ion in a LiCl–KCl molten on solid and liquid electrode. J Electroanal Chem 682:128–135
21. Li H, Kobrak MN (2009) A molecular dynamics study of the influence of ionic charge distribution on the dynamics of a molten salt. J Chem Phys 131:194507